Hybrid approximation spaces for solving the compressible Navier-Stokes equations with high Reynolds number

*Fan Zhang, Jian Cheng, †Tiegang Liu
School of Mathematics and Systems Science,
Beihang University, Beijing 100191, PR China.
*Presenting author: nmsdzf90@163.com
†Corresponding author: liutg@buaa.edu.cn

Abstract
Boundary layer will be produced if the Reynolds number of the compressible Navier-Stokes equations is sufficiently high. As there has a steep gradient of flow variables inside the boundary layer, it is very difficult to compute the Navier-Stokes equations stably and accurately. There are mainly two approaches to solve this problem. One is to use a very fine mesh whose grid size is approximate to the thickness of boundary layer. However, for the high dimensional problem, this may lead to an unbearable computing cost. The other is to use a high order numerical method, such as the Runge-Kutta discontinuous Galerkin (RKDG) method. However, as the thin thickness and large slope of the boundary layer, the traditional high order RKDG methods based on piecewise polynomial basis functions may not provide the best approximation to the solution and normal derivative inside the boundary layer unless a very fine spatial grid is divided.
In this paper, we consider the one-dimensional compressible Navier-Stokes equations which has an analytic solution under some assumptions, and according to its analytic solution, we provide an exponential approximation space for solving the computing domain inside the boundary layer. And for the computing domain outside the boundary layer, we still use the traditional polynomial space to approximate it. From numerical experiments we can see that compared to the traditional RKDG method based on polynomial approximation space, the RKDG method based on the hybrid approximation space provided in this paper can yield better results of the flow field values and gradient values over the same computing grid.

Keywords: Compressible Navier-Stokes equations, boundary layer theory, discontinuous Galerkin method, approximation space, exponential basis functions

Introduction
Flows of fluids with low viscosity values and thus very high Reynolds numbers occur in many technical applications. When a viscous fluid flows along a fixed impermeable wall, or past the rigid surface of an immersed body, an essential condition is that the velocity at any point on the wall or other fixed surface is zero. The extend to which this condition modifies the general character of the flow depends upon the value of the viscosity. If the body is of streamlined shape and if the viscosity is small without being negligible, which leads to a large value of Reynolds number, the modifying effect appears to be confined within narrow regions adjacent to the solid surfaces which are called as boundary layers [1]. Within such layers the fluid velocity changes rapidly from zero to its main-stream value, and this may imply a steep gradient of shearing stress. As a consequence, not all the viscous terms in the equation of motion will be negligible, even though the viscosity, which they contain as a factor, is itself very small.
The concept and theory of boundary layers have been developed by Ludwig Prandtl and presented in a historic paper in 1905 [2]. After then, physicists and engineers have written hundreds of articles and books about various aspects of boundary layer theory. And the most classic and best-known is Hermann Schlichting's boundary layer theory [3, 4]. The main characteristic of

the boundary layer theory is that the solution for the in-viscid outer flow and the solution for the boundary layer are being determined separately and matched properly, that is the flow region can be divided into two parts:

- Away from the surface of the object, viscous effects can be considered negligible, and potential flow can be assumed.
- In a thin region near the surface of the object, viscous effects cannot be neglected, and are as important as inertia.

Prandtl's boundary layer theory had a tremendous effect on the development of fluid mechanics and had attracted the attention of many researchers in finding high order numerical method to solve the the complete equations of motion of a viscous fluid - Navier-Stokes equations.
As there exist a large velocity gradient normal to the boundary in a very thin layer, it is considerably difficult to resolve it. One approach to solve this problem is mesh fitting. Because the accuracy of the numerical solutions are determined to some extent by the quality of the computing mesh, in order to obtain accurate solutions it would need to take a very fine mesh. Many researchers have worked in the field of performance and generation of boundary layer elements for CFD simulations. Karman presented a linear-elastic smoothing scheme to push bulk mesh and generate a new, unstructured viscous layer of elements [5–9]. The main idea of all these methods is to take a directional grid refinement procedure for accurate solution for the boundary layer and wake flow regions [10]. However, for high dimensional flow problems, this may lead to an unbearable computational cost and a low computing efficiency. Taking the two dimensional flat plate problem as an example, approximately 75% of the grid points are inside the boundary layer, which decrease the efficiency of numerical computing severely.
Another approach to obtain an accurate solution inside the boundary layer is to take a high order method, such as the finite difference method, finite volume method and finite element method, see review paper [11]. As the higher order the numerical method is, the larger number of solution unknowns or degrees of freedom are needed, this approach also brings a tremendous amount of computing. For the simulation of high dimensional turbulent flow problems, systems of several million degrees of freedom are common. Unfortunately, grid convergence, and hence reliable accuracy, is not always attained. What's more, high order methods applied to non-linear problems tend to become unstable when the approximating apace is inadequate to resolve the main features of the true solution. Unresolved boundary layers produce Gibbs oscillations which, in the presence of non-linearly, often lead to solution blow up [12].
Since the Navier-Stokes equations consist of the Euler equations plus shear-stress and heat flux terms, one of the major differences that occurs when solving the Navier-Stokes equations, as compared to the Euler equations, is the need to use fine meshes or high order scheme in order to properly resolve viscous layers. As the property of easily handling complex geometries and boundary conditions and achieving high order accuracy, the finite element method, especially the discontinuous Galerkin (DG) methods have received much attention during the last decade due to their ability to produce stable and high order accurate discretizations of conservation laws on fully unstructured meshes [13]. The DG method is a finite element method using a completely discontinuous piecewise polynomial space for the numerical solution and the test functions [14, 15]. The major development of DG methods was carried out by Cockburn and Shu in a series of papers [16–20]. They constructed high order Runge-Kutta discontinuous Galerkin (RKDG) method for the scaled conservation laws. And then this method was extended to one-dimensional and multi-dimensional systems.
When DG methods are used to solve partial differential equations (PDEs), the piecewise polynomial space is the commonly chosen finite element approximation space. However, for some

PDEs and initial/boundary conditions, piecewise polynomials may not provide the best approximation to the solution if the mesh is coarse, such as the Navier-Stokes equations with high Reynolds number [21]. And for the DG method based on non-classical piecewise polynomial basis functions, it has been studied in several literatures. In [22], Li and Shu proposed the use of locally divergence-free polynomial space in the DG method to solve the Maxwell equations and they achieved better results compared to the DG method based on the classical piecewise polynomial space P^k. Subsequently, the locally divergence-free polynomial space for approximating MHD equations, Hamilton-Jacobi equations and Laplace equation were discussed in [23–25]. However, these locally divergence-free polynomial space is still based on polynomials. Then in [26], Yuan and Shu developed discontinuous Galerkin methods based on non-polynomial approximation space, such as exponential approximation space and trigonometric approximation space, etc., for numerically solving time-dependent hyperbolic and parabolic and steady state hyperbolic and elliptic partial differential equations. However, this paper only discussed the scalar equation and what's more, the non-polynomial approximation space proposed in this paper was constructed without taking the analytic solution of the equation into account.

For the steady one-dimensional compressible Navier-Stokes equations, it can be solved analytically under the assumptions that the Prandtl number is taken as $\frac{3}{4}$ and the enthalpy is uniform on the boundaries [27]. As the analytic behaviour of the solution is available, the approximation of the solution can be improved by taking this information into account. Thus, in this paper, our main purpose is to propose a suitable approximation space which can approximate the Navier-Stokes equations accurately without needing to take a very fine mesh. Based on the traditional direct DG (DDG) method [28–30], we introduce a new DDG method based on a hybrid approximation space which is taken as an exponential approximation space inside the boundary layer and a polynomial approximation space outside the boundary layer in order to obtain a good approximation to the solutions over a coarse grid.

One-dimensional Compressible Navier-Stokes Equations

1. Non-dimensional compressible Navier-Stokes equations

The one-dimensional flow of viscous, heat-conducting, compressible fluid is described by the following hydrodynamic equations in conservative form

$$\frac{\partial Q}{\partial t} + \frac{\partial F}{\partial x} = \frac{\partial F_v}{\partial x}, \qquad x \in [x_L, x_R], \tag{1}$$

where $[x_L, x_R]$ is the solution domain, the conservation variable Q, the non-viscous flux F and the viscous flux F_v are defined as

$$Q = \begin{bmatrix} \rho \\ \rho u \\ E \end{bmatrix}, \quad F = \begin{bmatrix} \rho u \\ \rho u^2 + p \\ \rho u H \end{bmatrix}, \quad F_v = \begin{bmatrix} 0 \\ \tau_{xx} \\ u\tau_{xx} - q_x \end{bmatrix},$$

In order to make Eq.(1) closed, we also need an equation of state (EOS) and is assumed as

$$p = \rho R T. \tag{2}$$

Here,

$$\tau_{xx} = (2\mu + \lambda)\frac{\partial u}{\partial x}, \quad q_x = -k\frac{\partial T}{\partial x},$$

ρ is mass density, p is pressure, u is $x-$component of velocity. And in this paper, we assume the flow is from left to right, parallel to x-axis which means the velocity vector is positive. E is total energy per unit mass, H is enthalpy which is defined as

$$H = (E + p)/\rho = \frac{1}{2}u^2 + C_p T,$$

T is absolute temperature, μ is coefficient of viscosity and for simplicity we take it as a constant $\mu = \mu_r$. By using Stokes' hypothesis $\lambda = -\frac{2}{3}\mu$ the viscous stress τ_{xx} can be simplified to

$$\tau_{xx} = \frac{4}{3}\mu\frac{\partial u}{\partial x}.$$

k is the coefficient of thermal conductivity and is defined by

$$k = \frac{\mu C_p}{P_r},$$

in which P_r is the Prandtl number, $C_p = \dfrac{\gamma}{\gamma - 1}R$ is the specific heat at constant pressure, $\gamma = \frac{C_p}{C_v}$ is the ratio of specific heat, R is a gas constant which depends on the particular gas under consideration.
The boundary conditions of Eq.(1) are given as follows

$$\begin{cases} \rho(x_L) = \rho_L, \quad u(x_L) = u_L, \quad T(x_L) = T_L, \\ \rho(x_R) = \rho_R, \quad u(x_R) = u_R, \quad T(x_R) = T_R. \end{cases} \tag{3}$$

Next, we define the following dimensionless variables

$$\begin{aligned} & x = \frac{x^*}{L}, \quad u = \frac{u^*}{u_r}, \quad t = \frac{t^*}{L/u_r}, \\ & \rho = \frac{\rho^*}{\rho_r}, \quad p = \frac{p^*}{\rho_r u_r^2}, \quad T = \frac{T^*}{T_r}, \\ & R = \frac{R^*}{R_r}, \quad \mu = \frac{\mu^*}{\mu_r}, \\ & C_v = \frac{C_v^*}{U_r^2/T_r} = \frac{C_v^*}{\gamma \cdot R_r \cdot M_a^2} = \frac{1}{\gamma(\gamma-1)M_a^2}, \\ & C_p = \frac{C_p^*}{U_r^2/T_r} = \frac{C_p^*}{\gamma \cdot R_r \cdot M_a^2} = \frac{1}{(\gamma-1)M_a^2}, \\ & C_r = \sqrt{\gamma R_r T_r}, \quad u_r = M_a \cdot C_r, \end{aligned} \tag{4}$$

where the superscript * denotes the dimensional variables, subscript r denotes dimensional reference quantities and any non-marked variable denotes the non-dimensional variable. Then the non-dimensional form of (1) can be written as

$$\frac{\partial Q}{\partial t} + \frac{\partial F}{\partial x} = \frac{1}{Re}\frac{\partial F_v}{\partial x}. \tag{5}$$

Here, the forms of conservation variable Q, non-viscous flux F and viscous flux F_v are same

with those in Eq.(1). The Reynolds number which is defined as

$$R_e = \frac{\rho_r u_r L}{\mu_r},$$

significantly, corresponds to a non-dimensional reference length that directly controls the steepness of the non-dimensional gradients. Increasing R_e, as expected, thus leads to solutions that may be difficult to compute accurately.
The non-dimensional form of EOS (2) is

$$p = \rho T/(\gamma M_a^2) = \frac{\gamma - 1}{\gamma} C_p \rho T. \tag{6}$$

2. Analytic solution of the steady one-dimensional Navier-Stokes equations with $P_r = \frac{3}{4}$
For the non-dimensional Navier-Stokes equations (5), if the computing time is large enough, that is $t \to \infty$, it can be got that $\frac{\partial Q}{\partial t} \to 0$. Then we will have the steady one-dimensional compressible Navier-Stokes equations

$$\begin{cases} \dfrac{\partial \rho u}{\partial x} = 0, \\ \dfrac{\partial(\rho u^2 + p)}{\partial x} = \dfrac{1}{Re}\dfrac{\partial \tau_{xx}}{\partial x}, \\ \dfrac{\partial \rho u H}{\partial x} = \dfrac{1}{Re}\dfrac{\partial(u\tau_{xx} + \frac{\mu C_p}{P_r} T_x)}{\partial x}. \end{cases} \tag{7}$$

Integrating Eq.(7) once with respect to x in domain $[x_L, x]$, where x is any point in the whole computing domain $[x_L, x_R]$, leads to the following system

$$\begin{cases} \rho u = F_1, \\ \rho u^2 + p - \varepsilon\mu \frac{du}{dx} = F_2, \\ \rho u H - \varepsilon\mu(u\frac{du}{dx} + \frac{C_p}{\frac{4}{3}P_r}\frac{dT}{dx}) = F_3. \end{cases} \tag{8}$$

Here, $\varepsilon = \frac{4}{3}/R_e$ is a constant. And when the Reynolds number satisfies $R_e \to \infty$, we have $\varepsilon \to 0$. The constants $F_i\,(i = 1, 2, 3)$ are defined as

$$\begin{cases} F_1 = (\rho u)|_{x_L}, \\ F_2 = (\rho u^2 + p)|_{x_L}, \\ F_3 = (\rho u H)|_{x_L}. \end{cases} \tag{9}$$

According to [27], if we take the assumption that the Prandtl number is taken as $P_r = \frac{3}{4}$ and the coefficient of viscosity μ is taken as a constant, then the integrated Navier-Stokes equations (8) can be decoupled and simplified into a non-linear ordinary differential equation of velocity

$$\varepsilon\mu u\frac{du}{dx} - \frac{\gamma + 1}{2\gamma}F_1 u^2 + F_2 u - \frac{\gamma - 1}{\gamma}F_3 = \frac{\gamma - 1}{\gamma}F_1(H_R - H_L)e^{-F_1\frac{x_R - x}{\varepsilon\mu}}. \tag{10}$$

If the boundary conditions (3) satisfy $H_L = H_R$, then the equation of velocity (10) can be further reduced to

$$\varepsilon\mu u\frac{du}{dx} - \frac{\gamma + 1}{2\gamma}F_1 u^2 + F_2 u - \frac{\gamma - 1}{\gamma}F_3 = 0. \tag{11}$$

Eq.(11) can be solved analytically which leads to the following lemma

Lemma 1 *The solution of velocity of the steady one-dimensional compressible Navier-Stokes equations (7) under the assumptions that (i) $P_r = \frac{3}{4}$; (ii) $H_L = H_R$ is*

$$(u - u_0)(u - u_1)^{k_1} = (u_R - u_0)(u_R - u_1)^{k_1} \cdot e^{-k\xi}. \tag{12}$$

Here, $\xi = \frac{x_R - x}{\varepsilon\mu}$, u_0 and u_1 are the solutions which satisfy the non-viscous Rankine-Hugnoit relations

$$u_0 = u_L, \quad u_1 = (\frac{\gamma - 1}{\gamma + 1} + \frac{2}{\gamma + 1}\frac{1}{M_a^2})u_0. \tag{13}$$

$k = \frac{\frac{\gamma+1}{\gamma}F_1 u_0 - F_2}{u_0} > 0$ *and* $k_1 = -\frac{u_1}{u_0}$.

After obtaining the solution of velocity, by using the relationship between ρ and u

$$\rho u = F_1, \tag{14}$$

and the relationship between T and u

$$\frac{1}{2}u^2 + C_p T = H_L, \tag{15}$$

obtained from Eq.(8), we can obtain the complete solution of the steady one-dimensional Navier-Stokes equations (7).

From Eq.(12) we can see that when the Reynolds tends to infinity, that is the parameter ε tends to zero, the velocity in fact varies in the form of an exponential function in a thin region near the wall x_R. This region is called as boundary layer [2–4]. Outside the boundary layer, due to the exponential function $e^{-k\xi}$ on the right hand of the solution (12) closes to zero, the velocity remains as the constant u_L. Thus, the velocity varies rapidly inside the boundary layer from u_L to u_R which leads to an extremely large gradient value at the wall. And this usually cannot be calculated accurately by the traditional DG method based on polynomial approximation space unless a very fine mesh is used in numerical computing. However, for high dimensional problems, the cost of a very fine mesh is unbearable. Next, our main work is to construct a suitable non-polynomial approximation space for solving the one-dimensional compressible Navier-Stokes equations (5) with high Reynolds number inside the boundary layer in order to get a more accurate solution without needing to refine the computing mesh.

DDG Method Based on Hybrid Approximation Space

1. Hybrid approximation space for one-dimensional compressible viscous flow

The computational domain $[x_L, x_R]$ is divided into N cells with cell interfaces $x_L = x_{\frac{1}{2}} < x_{\frac{3}{2}} < \cdots < x_{N+\frac{1}{2}} = x_R$, and we denote the center of cell $I_j = [x_{j-\frac{1}{2}}, x_{j+\frac{1}{2}}]$ by x_j, and $\Delta x_j = x_{j+\frac{1}{2}} - x_{j-\frac{1}{2}}$ is the cell size of I_j. By dimensional analysis of the one-dimensional compressible Navier-Stokes equations (5), we can roughly estimate the thickness of the boundary layer δ has the same order of magnitude with $\frac{1}{R_e}$ [27]. Then according to the thickness of boundary layer δ and the cell size Δx, we can determine which computing cell is inside the boundary layer.

For the computing cells inside the boundary layer, from the solution (12), it can be seen that the solution of velocity is a linear combination of the following exponential functions

$$E_u = \{u : u \in span\{1, e^{-k\xi}, e^{-2k\xi}, e^{-3k\xi}, e^{-4k\xi}, \cdots\}, \xi = \frac{x_R - x}{\varepsilon\mu}\}. \tag{16}$$

Here, k is the same as defined in Lemma 1. Then according to the relationship between ρ and u (14) and the relationship between T and u (15), it can be seen that we can take the same

non-polynomial basis functions for approximating ρ and T with that for u (16).
Next, we consider the approximation space for conservative variables: ρ, ρu, E. For the energy variable E, we can take the approximation space of T (16) for solving it. For the momentum variable ρu, however, it should be noticed that, according to Eq.(8), as

$$\rho u = F_1 = const,$$

hence, we could just take the local orthogonal Legendre polynomial approximation space

$$P_{\rho u} = \{\rho u : \rho u \in span\{1,\, x - x_j,\, (x - x_j)^2 - \frac{1}{12}\Delta x^2,\, (x - x_j)^3 - \frac{3}{20}\Delta x^2 (x - x_j), \cdots\}\}$$

for solving it.
Thus the third order hybrid polynomial and exponential approximation space which is denoted as H^2 for solving the conservative variables inside the boundary layer are given as follows

$$H_0^{(j)}(x) = \begin{bmatrix} 1 \\ 1 \\ 1 \end{bmatrix}, \quad H_1^{(j)}(x) = \begin{bmatrix} e^{-k\frac{x_R - x}{\varepsilon\mu}} \\ x - x_j \\ e^{-k\frac{x_R - x}{\varepsilon\mu}} \end{bmatrix}, \quad H_2^{(j)}(x) = \begin{bmatrix} e^{-2k\frac{x_R - x}{\varepsilon\mu}} \\ (x - x_j)^2 - \frac{1}{12}\Delta x^2 \\ e^{-2k\frac{x_R - x}{\varepsilon\mu}} \end{bmatrix}. \quad (17)$$

And for the computing cells outside the boundary layer, we still use the third order Legendre polynomial approximation space P^2

$$P_0^{(j)}(x) = \begin{bmatrix} 1 \\ 1 \\ 1 \end{bmatrix}, \quad P_1^{(j)}(x) = \begin{bmatrix} x - x_j \\ x - x_j \\ x - x_j \end{bmatrix}, \quad P_2^{(j)}(x) = \begin{bmatrix} (x - x_j)^2 - \frac{1}{12}\Delta x^2 \\ (x - x_j)^2 - \frac{1}{12}\Delta x^2 \\ (x - x_j)^2 - \frac{1}{12}\Delta x^2 \end{bmatrix}. \quad (18)$$

Next, we will briefly conclude the steps for implementing the hybrid DDG method.

2. DDG method based on hybrid approximation space

The hybrid DDG method for solving the one-dimensional compressible Navier-Stokes equations (5) is set up as follows

Step 1 For each computing cell I_j $(j = 1, 2, \cdots, N)$, determining whether it is inside the boundary layer region or not.

Step 2 If the computing cell is inside the boundary layer, multiplying Eq.(1) by the arbitrary test functions $H_l^{(j)}(x)$ $(l = 0, 1, 2)$ in (17), integrating over the interval I_j and then integrating by parts, we will obtain the weak formulation of this equation

$$\int_{I_j} Q_t H_l^{(j)} dx - \int_{I_j} V(Q) \frac{dH_l^{(j)}}{dx} dx + \Delta_+ [V(Q_{j-\frac{1}{2}}) H_l^{(j)}(x_{j-\frac{1}{2}})] = 0, \quad (19)$$

where $\Delta_+ w_j = w_{j+1} - w_j$, $V(Q) = F(Q) - F_v(Q)$ and $Q_{j+\frac{1}{2}} = Q(x_{j+\frac{1}{2}})$. And if the computing cell is outside the boundary layer, the test functions will be changed to the second order Legendre polynomial functions $P_l^{(j)}(l = 0, 1, 2)$ in (18).

Step 3 For the computing cells inside the boundary layer, defining the degrees of freedom as

$$Q_j^{(l)} = Q_j^{(l)}(t) = \int_{I_j} Q(x, t) H_l^{(j)}(x) dx, \quad l = 0, 1, 2, \quad (20)$$

and

$$Q^h(x,t) = \sum_{l=0}^{2} A_l Q_j^{(l)}(t) H_l^{(j)}(x) \quad for \quad x \in I_j, \tag{21}$$

in which $A_l = \dfrac{1}{\int_{I_j}(H_l^{(j)}(x))^2 dx}$ and $Q^h(x,t)$ is the approximation of the solution $Q(x,t)$ in H^2.

Then replacing the solution Q by Q^h and taking it into Eq.(19), we will arrive at an ODE which are the degrees of freedom $Q_j^{(l)}$ $(l = 0, 1, 2)$ must satisfy

$$\frac{d}{dt}Q_j^{(l)} + \Delta_+[\widehat{V}_{j-\frac{1}{2}} H_l^{(j)}(x_{j-\frac{1}{2}})] - \int_{I_j} V(Q^h(x,t)) \frac{d}{dx} H_l^{(j)}(x) dx = 0, \quad l = 0, 1, 2, \tag{22}$$

where the numerical flux $\hat{V}$ is defined as $\hat{V} = V(Q^h, Q_x^h)$.

Similarly, if the computing cell is outside the boundary layer, the test functions will be changed to the Legendre polynomial functions $P_l^{(j)}(l = 0, 1, 2)$ (18) instead.

Step 4 For the numerical flux $\widehat{V}_{j+\frac{1}{2}} = \widehat{F}_{j+\frac{1}{2}} - \frac{1}{R_e} \cdot \widehat{F_v}_{j+\frac{1}{2}}$, we use the Lax-Friedrichs scheme

$$\begin{aligned} \widehat{F}_{j+\frac{1}{2}} &= F(Q^+_{j+\frac{1}{2}}, Q^-_{j+\frac{1}{2}}) \\ &= \frac{1}{2}[F(Q^+_{j+\frac{1}{2}}) + F(Q^-_{j+\frac{1}{2}}) - \alpha(Q^+_{j+\frac{1}{2}} - Q^-_{j+\frac{1}{2}})], \end{aligned}$$

where $\alpha = max|F'(Q)|$, to achieve total variation stability. And for the derivative term Q_x in $\hat{F}_v$, we use the piecewise linear approximation proposed in DDG method [28–30] to calculate it

$$\widehat{Q_x} = \beta_0 \frac{[Q]}{\Delta x} + \overline{Q_x}. \tag{23}$$

Here, $[Q] = Q^+ - Q^-$, $\overline{Q} = \frac{1}{2}(Q^+ + Q^-)$ and β_0 is a constant which is commonly taken as $\frac{1}{2}$.

Step 5 For the term of time, we use the third order Runge-Kutta scheme [13]

$$\begin{cases} u^{(1)} = u^n + \Delta t L(u^n), \\ u^{(2)} = \dfrac{3}{4}u^n + \dfrac{1}{4}u^{(1)} + \dfrac{1}{4}\Delta t L(u^{(1)}), \\ u^{n+1} = \dfrac{1}{3}u^n + \dfrac{2}{3}u^{(2)} + \dfrac{2}{3}\Delta t L(u^{(2)}). \end{cases} \tag{24}$$

Numerical results

Example 1. We solve the non-dimensional compressible Navier-Stokes equations (5) in $[0, 1]$ with the Reynolds number equals to 1.0×10^4. And the initial and boundary conditions are given as follows.

- Boundary condition

$$\begin{cases} u_L = 1.0, & u_R = 1.3, \\ \rho_L = 1.0, & \rho_R = (\rho_L \cdot u_L)/u_R, \\ T_L = 1.0, & T_R = (\frac{1}{2}u_L^2 + C_p T_L - \frac{1}{2}u_R^2)/C_p. \end{cases} \tag{25}$$

- Initial condition

$$\rho(x,0) = \begin{cases} \rho_L, & x \le x_B \\ \rho_L + \dfrac{x - x_L}{x_R - x_L}(\rho_R - \rho_L), & x > x_B, \end{cases}$$

$$u(x,0) = \begin{cases} u_L, & x \le x_B, \\ u_L + \dfrac{x - x_L}{x_R - x_L}(u_R - u_L), & x > x_B, \end{cases}$$

$$T(x,0) = \begin{cases} T_L, & x \le x_B, \\ T_L + \dfrac{x - x_L}{x_R - x_L}(T_R - T_L), & x > x_B. \end{cases}$$

Dividing the computing domain $[0,1]$ into $N = 800$ cells and taking $x_B = x_{N-3}$, then we use the DDG method based on standard P^2 polynomial basis functions ($DDG - P^2$), and DDG method based on hybrid basis functions ($DDG - H^2$) which is taken as P^2 basis functions (18) in the cells $i \le N-1$ and H^2 basis functions (17) in the cell $i = N$ to solve this equation, respectively, then compare the numerical results with the analytic solution (12). The results are shown in the following figure and table.

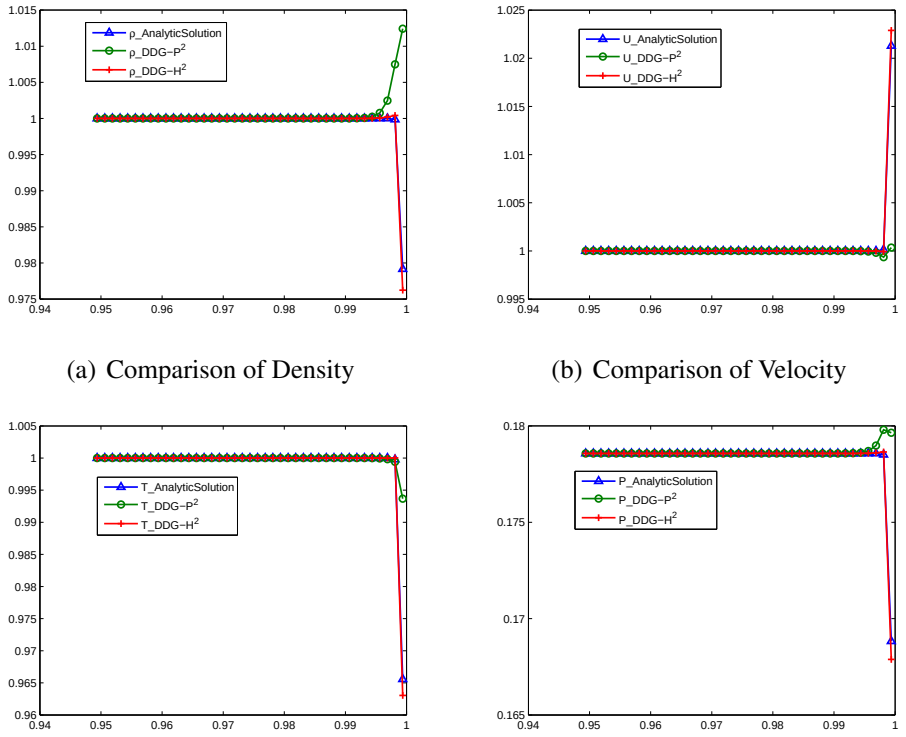

(a) Comparison of Density

(b) Comparison of Velocity

(c) Comparison of Temperature

(d) Computing error of Velocity

Figure 1: Example 1: Comparison of $DDG - P^2$ & $DDG - H^2$ with analytic solution.

Table 1: Example 1: Computing errors of flow variables (L_∞).

Error / Method	ρ	U	T	P
$DDG-P^2$	0.0333	0.0209	0.0281	0.0108
$DDG-H^2$	0.0029	0.0016	0.0025	0.0009

From Fig. 1 and Tab. 1 we can see that as the grid size we take is not small enough compared to the thickness of boundary layer, as expected, the traditional $DDG-P^2$ gives a poor flow variables profile. The flow field values outside the boundary layer might be correct but inside the boundary layer, they are obviously inaccurate and even have numerical oscillations. However, from Fig. 1 and Tab. 1 it can be seen that although we only change the basis functions in one computing cell $i=N$, the numerical results computed by the $DDG-H^2$ method proposed in this paper are very close to the analytic solution everywhere.

As mentioned above, because the Reynolds number taken in this example is very high, there have a steep gradients of flow variables near the wall, and these gradient values have an important effect on computing the coefficient of skin friction and other physical quantities in high dimensional problems. Thus, next, we will compare the numerical results of gradient values at the wall x_R.

Table 2: Example 1: Percentage errors of gradient values at the wall x_R.

Error(%) / Method	ρ_x	u_x	T_x	P_x
$DDG-P^2$	26.1745	41.8165	45.2866	38.7611
$DDG-H^2$	1.1076	2.0544	3.3219	2.6517

It is obvious to see from Tab. 2 that, under the same computing grid, although it seems that the numerical results computed by $DDG-P^2$ method are acceptable from the point of L_∞ computing error, but it gives poor approximation for the gradient values of flow variables at the wall x_R. However, the $DDG-H^2$ method is far more effective than the $DDG-P^2$ method in computing the gradient values and it can provide a very accurate approximation results.

Example 2. We also solve Eq.(5) with the same boundary and initial conditions with those of Example 1. We increase the number of computing grids N to 1600, 2400 and 3200, respectively, and compute the gradients of flow variables at the wall x_R by the $DDG-P^2$ method again to see the variations of percentage errors with the number of grids. The results are shown in the following table.

Table 3: Example 2: Percentage errors of gradient values at the wall x_R ($DDG - P^2$).

Error(%) / N	ρ_x	u_x	T_x	P_x
800	26.1745	41.8165	45.2866	38.7611
1600	7.4528	17.4923	16.9579	13.9999
2400	2.5276	8.7675	7.2083	5.8779
3200	0.9195	5.0338	3.4916	2.8179

From Tab. 3 we can see that the percentage errors of gradient values are decreasing slowly with the grid size becoming smaller. We can also that compared to the $DDG - H^2$ method, the $DDG - P^2$ method should take nearly four times the number of grids more than that of the $DDG - H^2$ method does in order to obtain the same order of percentage errors. And this, from the other perspective, demonstrate that the DDG method based on hybrid basis functions (17) is effective in decreasing the number of grids needed in solving the Navier-Stokes equations with high Reynolds number and can obtain a very accurate result of gradient value on a coarse mesh. It can save nearly 75% of the grids number.

Example 3. Here, we use higher order accuracy methods: $DDG - P^3$ and $DDG - P^4$ methods to solve Example 1 on a coarse mesh ($N = 800$), then compare the numerical results with that of $DDG - H^2$ method, the comparisons are shown in the following table.

Table 4: Example 3: Percentage errors of gradient values at the wall x_R.

Error(%) / Method	ρ_x	u_x	T_x	P_x
$DDG - P^2$	26.1745	41.8165	45.2866	38.7611
$DDG - P^3$	4.6980	12.7386	11.0475	8.9381
$DDG - P^4$	0.3093	1.7141	2.1390	1.6020
$DDG - H^2$	1.1076	2.0544	3.3219	2.6517

It is obviously to see from Table 4 that, better results are obtained when using a high order DDG method based on polynomial basis functions (18). And it nearly needs to take fifth order accuracy DDG method based on the polynomial basis functions in order to obtain the same order of percentage errors with those of the $DDG - H^2$ method proposed in our paper.

Conclusions

The main objective of this paper is to propose a suitable non-polynomial approximation basis function for solving the compressible Navier-Stokes equation with high Reynolds number which has a thin boundary layer near the wall of object. According to the analytic solution of the one-dimensional steady compressible Navier-Stokes equations under the assumptions that the Prandtl number is taken as $\frac{3}{4}$ and the coefficient of viscosity is taken as a constant, we proposed a DDG method based on a hybrid exponential and polynomial approximation space for solving the Navier-Stokes equations. Numerical tests have shown compared to the DDG method based on the standard polynomial approximation space, the DDG method based on the hybrid approximation space proposed in this paper can obtain a more accuracy results, especially for

the gradients values of flow variables on the wall, with less number of degrees of freedom over a coarse grid. Further research focusing on high dimensional problems is on going.

References

1. I. MARUSIC, B. J. MCKEON, P. A. MONKEWITZ, H. M. NAGIB, A. J. SMITS, *Wall-bounded Turbulent Flows at High Reynolds Numbers: Recent Advances and Key Issues*, Physics of Fluids, 22(2010), pp. 065103.

2. L. PRANDTL, *Verhandlung des III Internationalen Mathematiker-Kongresses (heidelberg, 1904)*, A. Krazer, ed., Teubner, Leipzig, Germany 1905, pp. 484–491.

3. H. SCHLICHTING, *Boundary-layer Theory*, 7th ed., McGrawHill, New York, 1979.

4. TUNCER CEBECI, JEAN COUSTEIX, *Modeling and Computation of Boundary-layer Flows: Laminar, Turbulent and Transitional Boundary Layers in Incompressible and Compressible Flows (second revised and extended edition)*, Horizon Publishing, 2005.

5. KARMAN S. L., *Unstructured Viscous Layer Insertion Using Linear-elastic Smoothing*, AIAA Journal, 45(2007), pp. 168–180.

6. GUILLAUME V., FORNIER Y., AND BOUBEKEUR T, *Hybrid Viscous Layer Insertion in a Tetrahedral Mesh*, In IMR (Research Note), 2012.

7. ITO Y., NAKAHASHI K., *Unstructured Mesh Generation for Viscous Flow Computations*, IMR, 2002, pp. 367–377.

8. BAHRAINIAN S. S., MEHRDOOST Z., *An Automatic Unstructured Grid Generation Method for Viscous Flow Simulations*, Mathematics and Computers in Simulation, 2012.

9. GARIMELLA R. V., SHEPHARD M. S., *Boundary Layer Mesh Generation for Viscous Flow Simulations*, International Journal for Numerical Methods in Engineering, 49(200), pp. 193–218.

10. RAJEEV J., TIMOTHY J. T., *PostBL: Post-Mesh Boundary Layer Mesh Generation Tool*, In: Sarrate J., Staten M. (eds) Proceedings of the 22nd International Meshing Roundtable, Springer, Cham, 2014.

11. Z.J. WANG, *High-order Methods for the Euler and NavierCStokes Equations on Unstructured Grids*, Progress in Aerospace Sciences, 43(2007), pp. 1–41.

12. , *RANS Solutions Using High Order Discontinuous Galerkin Methods*, Aiaa Aerospace Science Meeting & Exhibit Reno for Discontinuous Galerkin, 2007.

13. B. COCKBURN, C. W. SHU,*Runge-Kutta Discontinuous Galerkin Methods for Convection-Dominated Problems*, Journal of Scientific Computing, 16 (2001) , pp. 173–261.

14. BERNARDO COCKBURN , GEORGE E. KARNIADAKIS AND CHI-WANG SHU,*The Development of Discontinuous Galerkin Methods*, 1999.

15. W. H. REED AND T. R. HILL, *Triangular Mesh Methods for the Neutron Transport Equation*, Tech.report LA-UR-73-479, Los Alamos Scientific Laboratory, Loa Alamos, NM, 1973.

16. B. COCKBURN, C. W. SHU, *TVB Runge-Kutta Local Projection Discontinuous Galerkin Finite Element Method for Scalar Conservation Laws II: General framework*, Math. Comp., 52 (1989), pp. 411–435.

17. B. COCKBURN, C. W. SHU, *TVB Runge-Kutta Local Projection Discontinuous Galerkin Finite Element Method for Scalar Conservation Laws III: One dimensional systems*, J. Comput. Phys., 84 (1989), pp. 90–113.

18. B. COCKBURN, C. W. SHU, *TVB Runge-Kutta Local Projection Discontinuous Galerkin Finite Element Method for Scalar Conservation Laws IV: The multidimensional case*, Math. Comp., 54 (1990), pp. 545–581.

19. B. COCKBURN, C. W. SHU, *The Runge-Kutta Local P^1 Discontinuous Galerkin Finite Element Method for Scalar Conservation Laws*, RAIRO Modél. Math. Comp., 52 (1989), pp. 411–435.

20. B. COCKBURN, G. E. KARNIADAKIS AND C.-W. SHU, *The Local Discontinuous Galerkin Method for Time-dependent Convection-diffusion Systems*, SIAM J. Numer. Anal., 35 (1998), pp. 2440–2463.

21. YUAN LING, C. W. SHU, *Discontinuous Galerkin Method Based on Non-polynomial Approximation Spaces*, J. Comput. Phys., 218 (2006), pp. 295–323.

22. B. COCKBURN, F. LI AND C.-W. SHU, *Locally Divergence-free Discontinuous Galerkin Methods for the Maxwell Equations*, Journal of Computational Physics, 194(2004), pp. 588–610.

23. F. LI, C.-W. SHU, *Locally Divergence-free Discontinuous Galerkin Methods for MHD Equations*, Journal of Scientific Computing, 22-23(2005), pp. 413-442.

24. F. LI, C.-W. SHU, *Reinterpretation and Simplified Implementiation of a Discontinuous Galerkin Method for Hamilton-Jacobi Equations*, Applied Mathematics Letters, 18(2005), pp. 1204–1209.

25. F. LI, C.-W. SHU, *A Local-structure-preserving Local Discontinuous Galerkin Method for the Laplace Equation*, Methods and Applications of Analysis, 2(2006), pp. 215-C234

26. L. YUAN, C.-W. SHU, *Discontinuous Galerkin Method Based on Non-polynomial Approximation Spaces*, Journal of Computational Physics, 218(2006), pp. 295–323.

27. FAN ZHANG, TIEGANG LIU, *Solutions of Steady One-dimensional Compressible Navierstokes Equations under Uniform Enthalpy with $P_r = \frac{3}{4}$*. (To appear)

28. HAILIANG LIU, JUE YAN, *The Direct Discontinuous Galerkin (DDG) Methods for Diffusion Problems*, SIAM J.Numer. Anal, 47 (2009), pp. 675–698.

29. JIAN CHENG, XIAOQUAN YANG, XIAODONG LIU, TEIGANG LIU AND HONG LUO, *A Direct Discontinuous Galerkin Method for the Compressible NavierCStokes Equations on Arbitrary Grids*, Journal of Computational Physics, 327(2016), pp. 484–502.

30. JIAN CHENG, XIAODONG LIU, TIEGANG LIU AND HONG LUO, *A Parallel, High-Order Direct Discontinuous Galerkin Method for the Navier-Stokes Equations on 3D Hybrid Grids*, Communications in Computational Physics, 21(2017), pp. 1231–1257.